J|A|C|S
ARTICLES
Published on Web 01/21/2004

Thermodynamics of Binding of 2-Methoxy-3-isopropylpyrazine and 2-Methoxy-3-isobutylpyrazine to the Major Urinary Protein

Richard J. Bingham,[†] John B. C. Findlay,[†] Shih-Yang Hsieh,[†] Arnout P. Kalverda,[†] Alexandra Kjellberg,[†] Chiara Perazzolo,[‡] Simon E. V. Phillips,[†] Kothandaraman Seshadri,[†] Chi H. Trinh,[†] W. Bruce Turnbull,[†] Geoffrey Bodenhausen,[‡] and Steve W. Homans*,[†]

Contribution from the Astbury Centre for Structural Molecular Biology, School of Biochemistry & Molecular Biology, University of Leeds, LS2 9JT Leeds, UK, and Institut de Chimie Moleculaire et Biologique, Ecole Polytechnique Federale de Lausanne (EPFL), BCH 1015 Lausanne, Switzerland

Received September 11, 2003; E-mail: s.w.homans@leeds.ac.uk

Abstract: In the present study we examine the thermodynamics of binding of two related pyrazine-derived ligands to the major urinary protein, MUP-I, using a combination of isothermal titration calorimetry (ITC), X-ray crystallography, and NMR backbone ^{15}N and methyl side-chain ^{2}H relaxation measurements. Global thermodynamics data derived from ITC indicate that binding is driven by favorable enthalpic contributions, rather than the classical entropy-driven hydrophobic effect. Unfavorable entropic contributions from the protein backbone and side-chain residues in the vicinity of the binding pocket are partially offset by favorable entropic contributions at adjacent positions, suggesting a "conformational relay" mechanism whereby increased rigidity of residues on ligand binding are accompanied by increased conformational freedom of side chains in adjacent positions. The principal driving force governing ligand affinity and specificity can be attributed to solvent-driven enthalpic effects from desolvation of the protein binding pocket.

Introduction

Protein−ligand interactions are of fundamental importance in a great many biological processes. However, despite enormous advances in the speed and accuracy of the three-dimensional structure determination of proteins and their complexes, our ability to predict binding affinity from structure remains severely limited. One reason for this dilemma is that affinities are governed not only by energetic considerations concerning the precise spatial disposition of interacting groups but also by the dynamics of these groups in addition to solvent effects. Thus, to predict accurately the affinity of a protein for a given ligand, it is essential to have prior knowledge of both the enthalpy of binding, ΔH_b°, and the entropy of binding, ΔS_b°. A quantitative measure of the elusive ΔS_b° component is notoriously difficult since it depends on the dynamics of the complex (including solvent) over all degrees of freedom of the system. Isothermal titration microcalorimetry experiments offer the possibility to measure thermodynamic binding parameters including ΔS_b°, but since the derived parameters are global in nature, it is difficult to separate contributions from protein, ligand, and solvent. In principle characterization of the internal dynamics of a protein in the absence and presence of ligand should enable measurement of ΔS_b° values associated with the internal degrees of freedom of the protein. In particular, NMR relaxation-time measurements offer scope for the measurement of ΔS_b° on a per-residue basis, and this approach has been pioneered by a number of workers.[1−4] Evidence to date suggests that NMR-derived ΔS_b° values can be correlated with values obtained from independent methods.[5,6]

In the present study we examine the entropies of binding of two related ligands, namely, 2-methoxy-3-isopropylpyrazine (IPMP) and 2-methoxy-3-isobutylpyrazine (IBMP), to the major urinary protein, MUP-I, using a combination of isothermal titration calorimetry (ITC), X-ray crystallography, and NMR backbone ^{15}N and methyl side-chain ^{2}H relaxation measurements.[7,8] While structurally very similar, in preliminary ITC measurements these ligands differed in affinity by approximately 1 order of magnitude, and hence offer an interesting model system to probe the thermodynamics of both affinity and specificity of the protein. MUP-I is one of a series of variants of the major urinary protein, which is an abundant pheromone-binding protein found in male mouse urine, where subtle recognition of a series of related compounds is essential to its

[†] University of Leeds.
[‡] EPFL Lausanne.

(1) Akke, M.; Brüschweiler, R.; Palmer, A. G. *J. Am. Chem. Soc.* **1993**, *115*, 9832−9833.
(2) Li, Z. G.; Raychaudhuri, S.; Wand, A. J. *Protein Sci.* **1996**, *5*, 2647−2650.
(3) Yang, D. W.; Kay, L. E. *J. Mol. Biol.* **1996**, *263*, 369−382.
(4) Yang, D.; Mok, Y.-K.; Forman-Kay, J. D.; Farrow, N.; Kay, L. E. *J. Mol. Biol.* **1997**, *272*, 790−804.
(5) Lee, A. L.; Kinnear, S. A.; Wand, A. J. *Nat. Struct. Biol.* **2000**, *7*, 72−77.
(6) Wrabl, J. O.; Shortle, D.; Woolf, T. B. *Proteins* **2000**, *38*, 123−133.
(7) Farrow, N. A.; Muhandiram, R.; Singer, A. U.; Pascal, S. M.; Kay, C. M.; Gish, G.; Shoelson, S. E.; Pawson, T.; Formankay, J. D.; Kay, L. E. *Biochemistry* **1994**, *33*, 5984−6003.
(8) Muhandiram, D. R.; Yamazaki, T.; Sykes, B. D.; Kay, L. E. *J. Am. Chem. Soc.* **1995**, *117*, 11536−11544.

10.1021/ja038461i CCC: $27.50

Chart 1

1	M	R	G	S	H	H	H	H	H	H	G	S	E*	E	A	S	S	T	G	R	N	F	N	V	E	K	I	N	G	E
31	W	H	T	I	I	L	A	S	D	K	R	E	K	I	E	D	N	G	N	F	R	L	F	L	E	Q	I	H	V	L
61	E	K	S	L	V	L	K	F	H	T	V	R	D	E	E	C	S	E	L	S	M	V	A	D	K	T	E	K	A	G
91	E	Y	S	V	T	Y	D	G	F	N	T	F	T	I	P	K	T	D	Y	D	N	F	L	M	A	H	L	I	N	E
121	K	D	G	E	T	F	Q	L	M	G	L	Y	G	R	E	P	D	L	S	S	D	I	K	E	R	F	A	Q	L	C
151	E	E	H	G	I	L	R	E	N	I	I	D	L	S	N	A	N	R	C	L	Q	A	R	E						

biological function.[9,10] The crystal structure of MUP-I isolated from urine was solved by Böcskei and co-workers.[11] The protein has a typical lipocalin fold that consists of an eight-stranded β-barrel and a single α-helix, and the interior of the barrel forms a hydrophobic cavity. A number of small hydrophobic molecules can bind within the cavity, and the protein is thus an ideal model system to study the entropic contribution to affinity and specificity. The resulting complexes are small enough (ca. 20 kDa) to permit detailed analysis by high-resolution NMR, and full assignments are available.[12] By comparing two ligands rather than a single ligand binding to MUP-I, we aim simultaneously to examine the contribution of $\Delta S_b°$ to both affinity and specificity of binding.

Materials and Methods

Preparation and Purification of MUP−I and ^{13}C,^{15}N(>97%),^{2}H-(50%)-MUP-I. Overexpression. The MUP-I gene was cloned into the pQE30 vector and overexpressed in *Escherichia coli* strain SG13009. A single colony from an agar plate containing 50 μg/mL ampicillin and 10 μg/mL kanamycin was inoculated into 10 mL of LB medium containing 50 μg/mL ampicillin for overnight culture at 37 °C. Five milliliters of this culture was used to seed 500 mL of LB medium containing 50 μg/mL ampicillin in 2-L flasks. In the case of ^{13}C,^{15}N-(>97%),^{2}H (50%)-MUP-I expression, LB medium was substituted with Celtone dCN (>97% ^{13}C, ^{15}N, 50% ^{2}H, Spectra Stable Isotopes, Columbia Md). Expression was induced by addition of isopropyl-thiogalactoside to a final concentration of 1 mM when culture density reached OD_{600} 0.6−0.8. After a 6 h induction, cells were harvested by centrifugation at 5000*g* for 15 min. The pellet was suspended in 5 mL of phosphate-buffered saline (PBS, pH 7.4, 5 mL/gram wet weight) containing 0.16 mg/mL lysozyme, and the suspension was stirred for 20 min, followed by addition of 4 mg of deoxycholic acid per gram of wet pellet. Following incubation at 37 °C until the solution became viscous, 20 μL of 1 mg/mL stock solution of DNase I was added per gram wet weight pellet, followed by further incubation at 37 °C until the solution was no longer viscous. The resulting lysate was centrifuged at 5000*g*, and the supernatant was retained for further purification.

Purification. MUP-I was purified using Ni−NTA resin (Qiagen). To remove endogenous bound ligands, an ethanol precipitation step was utilized involving addition of 2 volumes of absolute ethanol per volume of protein solution, followed by incubation at 4 °C for 2 h. After centrifugation at 5000*g*, the pellet was lyophilised, resuspended in PBS pH 7.4, and dialyzed overnight against the same buffer. The sequence of the expressed protein was confirmed by mass spectrometry as shown in Chart 1. Throughout this work the residue numbering of Abbate et al. was used,[12] i.e., residue 1 (marked with an asterisk) corresponds with the first residue of the mature protein sequence.

NMR Measurements. All NMR measurements were performed at pH 7.4 and a temperature of 308 K at a proton frequency of 600 MHz. ^{15}N relaxation-time measurements were acquired essentially according to Farrow et al.[7] Amide ^{15}N T_1 relaxation times were acquired on ^{15}N,^{13}C(>97%),^{2}H(50%)-enriched protein at a sample concentration of 1 mM with relaxation delays of 10.9, 54.3, 108.6, 217.3, 434.6, 651.8, 923.4, 1249.4, and 1629.6 ms, and T_2 relaxation times were acquired with relaxation delays of 16.7, 33.4, 50.1, 66.8, 83.5, 100.2, 133.6, and 167.0 ms. Methyl ^{2}H T_1 and $T_{1\rho}$ relaxation time measurements[8] were acquired on methyl $^{13}CH_2D$ isotopomers in the same sample, using relaxation delays of 1.2, 4, 8, 14, 22, 32, 46, 60 ms and 1.2, 2.4, 4, 6, 9, 12, 16, and 22 ms, respectively. The radio frequency ^{2}H spin-lock field strength for $T_{1\rho}$ measurements was 1 kHz. Aliquots of the same protein sample were used to acquire similar data sets for complexes of MUP-I with IPMP and IBMP, after addition of a 5-fold molar excess of each ligand. In all cases data were fit to single exponential decays, and the resulting decay rates were interpreted in terms of the Lipari−Szabo model-free spectral density[13] using the MODELFREE software package[14] kindly provided by Professor Art Palmer (Columbia University) in the case of ^{15}N relaxation data, or using a software package kindly provided by Dr. Neil Farrow in the case of ^{2}H relaxation data. A global rotational correlation time of 8.57 ns with isotropic rotational tumbling was used for these calculations, according to a previous report.[9] Errors in S^2 values were estimated by Monte Carlo simulations as implemented in the MODELFREE package. In all cases good fits were obtained without a contribution from exchange broadening R_{ex}.

X-ray Crystallography. Crystallization and Data Collection. Optimal conditions for crystallization of 55 mM CdCl, 100 mM malate buffer, pH 4.9, 18 °C were based on previously identified conditions.[11] Drops containing 1 μL of MUP-I (10 mg/mL) and 1 μL of reservoir solution were equilibrated against reservoir solution by vapor diffusion using the hanging drop method. Crystals of space group $P4_32_12$ grew over a period of 3−7 days. Ligand soaks were conducted by the addition of neat ligand (IPMP or IBMP) to the reservoir solution to a final concentration of 12 μM. This was then allowed to equilibrate with the drop for 24−48 h. After soaking for 1 min in a cryoprotecting solution consisting of reservoir solution with the addition of 20% (v/v) glycerol and 12 μM ligand, crystals were flash-frozen in liquid nitrogen. Data collection of apo-MUP-I was conducted at Daresbury synchrotron source (station 14.1, U.K.). Data collection of ligand soaked crystals was conducted on the laboratory X-ray source, which consisted of a rotating anode generator (RU-H3R, Rigaku), Confocal Max-Flux optics (Osmic), and an R-axis IV++ (Rigaku) image plate detector. In both cases the crystals were maintained at 100 K by a cryostream (Oxford Cryosystems). Data collection details are shown in Table 1. Data were processed and scaled using the programs MOSFLM version 6.10,[15] and SCALA.[16]

Structure Determination by Molecular Replacement. The structure of MUP-I (PDB accession number 1I06) with all water molecules and bound ligand removed, was used as the molecular replacement trial model. AMoRe[17] was used to conduct the rotation and translation searches and initial rigid body refinement stage resulting in an initial R_{cryst} of 40%. After several rounds of automatic positional and thermal factor refinement using CNS[18] interspersed with manual remodeling in the program "O",[19] the final statistics shown in Table 1 were produced. Cadmium ions are known to be involved in crystal contacts

(9) Zidek, L.; Novotny, M. V.; Stone, M. J. *Nat. Struct. Biol.* **1999**, *6*, 1118−1121.
(10) Zidek, L.; Stone, M. J.; Lato, S. M.; Pagel, M. D.; Miao, Z. S.; Ellington, A. D.; Novotny, M. V. *Biochemistry* **1999**, *38*, 9850−9861.
(11) Bocskei, Z.; Groom, C. R.; Flower, D. R.; Wright, C. E.; Phillips, S. E. V.; Cavaggioni, A.; Findlay, J. B. C.; North, A. C. T. *Nature* **1991**, *360*, 186−188.
(12) Abbate, F.; Franzoni, L.; Lohr, F.; Lucke, C.; Ferrari, E.; Sorbi, R. T.; Ruterjans, H.; Spinsi, A. *J. Biomol. NMR* **1999**, *15*, 187−188.
(13) Lipari, G.; Szabo, A. *J. Am. Chem. Soc.* **1982**, *104*, 4546−4559.
(14) Mandel, A. M.; Akke, M.; Palmer, A. G. *J. Mol. Biol.* **1995**, *246*, 144−163.
(15) Leslie, A. G. W. In *CCP4 & ESFEACMB Newsletter On Protein Crystallography*; Daresbury Laboratory: Warington, 1992.
(16) CCP4 In *Acta Crystallogr.* **1994**, *D50*, 760−763.
(17) Navaza, J. *Acta Crystallogr. Sect. A* **1994**, *50*, 157−163.

Table 1. Data Collection and Processing Statistics[a]

	free protein	IPMP complex	IBMP complex
wavelength (nm)	0.149	0.154	0.154
resolution range (nm)	2.5−0.18	2.8−0.175	2.8−0.17
unique reflections	18699	20419	14995
completeness (%)	93.1	98.1	91.5
multiplicity	5.5	6.8	6.1
R_{sym}[b]	0.090 (0.22)	0.083 (0.35)	0.065 (0.21)
unit cell dimensions (nm)	$a = b = 5.36$ $c = 13.70$	$c = 13.77$	$a = b = 5.36$ $c = 13.76$
R_{work} (R_{free})	17.7 (21.9)	18.3 (20.6)	18.1 (21.0)
rmsd from ideal:			
bond length (nm)	0.0017	0.0018	0.0018
angles (deg)	1.76	1.8	1.81

[a] Space group for all crystals was $P4_32_12$. [b] Values in parentheses are for highest resolution shell. $R_{sym} = \sum_{hkl}\sum_i(I_i(hkl) - I_{mean}(hkl))/\sum_{hkl}\sum_i(I_i(hkl))$.

from previous studies[20] and were easily identified as large peaks on the electron density maps. CNS topology and parameter files for IPMP and IBMP were generated automatically by PRODRG.[21] The crystallographic model does not include all residues of the protein. Twelve N-terminal residues including the hexa-His tag, and eight C-terminal residues were not resolvable due to weak electron density. The refined crystallographic models resulted in high-quality electron density maps for all structures. The main chain torsion angles for all residues lie in allowed regions of a Ramachandran plot with the single exception of Tyr115.[22] Crystal coordinates have been deposited in the RCSB protein databank, accession numbers 1QY0, 1QY1, and 1QY2.

Isothermal Titration Calorimetry (ITC) Measurements. ITC experiments were conducted using a MicroCal VP-ITC unit operating at 308 K. Prior to use, the protein was precipitated with ethanol to remove any endogenous ligands and then redissolved, dialyzed against PBS (pH 7.4), and degassed in vacuo. The ligands were dissolved in degassed PBS, and all concentrations were measured by UV absorption (MUP-I $\epsilon_{280} = 10\ 650\ M^{-1}\ cm^{-1}$; IBMP $\epsilon_{220} = 4980\ M^{-1}\ cm^{-1}$; IPMP $\epsilon_{220} = 4600\ M^{-1}\ cm^{-1}$) immediately prior to starting the titrations. IBMP and IPMP experiments used protein concentrations of ca. 20 and 30 μM, respectively. Titrations were performed in duplicate and typically comprised 25 injections ($1 \times 2\ \mu$L followed by $24 \times 5\ \mu$L) at 4 min intervals. The initial data point was routinely deleted to allow for diffusion of ligand/receptor across the needle tip during the equilibration period. Heats of dilution for each ligand were measured independently and subtracted from the integrated data prior to curve fitting in Origin 5.0 with the standard One Site model supplied by MicroCal which is based on the Wiseman isotherm:[23,24]

$$\frac{dQ}{d[X]_t} = \Delta H^\circ V_0\left[\frac{1}{2} + \frac{1 - X_R - r}{2\sqrt{(1 + X_R + r)^2 - 4X_R}}\right]$$

where, $dQ/d[X]_t$ is the stepwise change in heat of the system normalized with respect to the change in the total concentration of the ligand ($[X]_t$), ΔH° is the standard enthalpy for reaction, V_0 is the effective volume of the calorimeter cell, X_R is the ratio of the total ligand to receptor concentrations at any given point during the titration, and r is defined by:

$$\frac{1}{r} = nK_a[M]_t$$

wherein n is the number of binding sites per protein molecule, K_a is the association constant, and $[M]_t$ is the total protein concentration.

Results and Discussion

Crystal Structures of MUP-I Complexes. To enable a structure-based interpretation of the thermodynamic measurements that follow, the crystal structures of MUP-I both alone and in complex with IPMP and IBMP were solved, and data collection and processing statistics are shown in Table 1.

The apo protein was found to contain electron density in the binding pocket that was modeled as a single molecule of glycerol from the cryoprotectant. In the pyrazine complexes, both ligands are bound in similar orientations within the β-barrel, in a hydrophobic environment formed by the side chains of Phe 38, Leu 40, Leu 42, Ile 45, Leu 54, Phe 56, Met 69, Val 82, Tyr 84, Phe 90, Ala 103, Leu 105, Leu 116, and Tyr 120 (Figure 1—residue numbering follows that of Abbate et al.[12]). In contrast to the crystal structure of MUP-I in complex with the natural pheromones 2-*sec*-butyl-4,5-dihydrothiazole and 6-hydroxy-6-methyl-3-heptanone,[25] no water molecules are found in the binding site of the pyrazine complexes. Instead, Tyr 120 hydroxyl group hydrogen bonds directly to one of the ring nitrogens in each ligand. There are no significant conformational differences in the protein backbone between the two pyrazine complexes (overall mean global backbone rmsd = 0.007 nm), and with the exception of Leu 116 which is located in the binding site, only minor differences are observed for side-chain atoms (overall mean global side-chain rmsd = 0.035 nm).

ITC Measurements. To facilitate an overall assessment of the global thermodynamics of binding of IBMP and IPMP to MUP-I, isothermal titration calorimetry experiments were performed at 308 K. Typical isotherms are shown in Figure 2, and the resulting thermodynamic parameters are shown in Table 2.

It can be seen that both ligands bind with affinities in the micromolar range, in a process that is largely enthalpy driven. IBMP binds approximately 6-fold more strongly than IPMP, due to more favorable contributions from both binding enthalpy (ΔH_b) and binding entropy (ΔS_b). The binding site of MUP-I is very hydrophobic, and given that only one ligand−protein hydrogen bond is formed in each complex, namely between the hydroxyl group of Tyr 120 and a ring nitrogen, an entropy-driven binding process would at first sight be anticipated. These observations highlight the limitations of global thermodynamic parameters for investigating biomolecular recognition processes in molecular detail.

Backbone ^{15}N Relaxation Measurements. To gain deeper insight into the entropic contribution to binding of both IPMP and IBMP, we utilized NMR relaxation measurements to probe per-residue configurational entropies at backbone amide and

(18) Brünger, A. T.; Adams, P. D.; Clore, G. M.; DeLango, W. L.; Gros, P.; Grosse-Kunstleve; R. W. Jiang, J.-S.; J., K.; Nilges, M.; Pannu, N. S.; Read, R. J.; Rice, L. M.; Simonson, T.; Warren, G. L. *Acta Crystallogr.* **1998**, *D54*, 905−921.
(19) Jones, T. A.; Zou, J. Y.; Cowan, S. W.; Kjeldgaard, M. *Acta Crystallogr., Sect. A* **1991**, *47*, 110−119.
(20) Bocskei, Z.; Groom, C. R.; Flower, D. R.; Wright, C. E.; Phillips, S. E. V.; Cavaggioni, A.; Findlay, J. B. C.; North, A. C. T. *Nature* **1992**, *360*, 186−188.
(21) vanAalten, D. M. F.; Bywater, R.; Findlay, J. B. C.; Hendlich, M.; Hooft, R. W. W.; Vriend, G. *J. Comput-Aided Mol. Des.* **1996**, *10*, 255−262.
(22) Laskowski, R. A.; MacArthur, M. W.; Moss, D. S.; Thornton, J. M. *J. Appl. Crystallogr.* **1993**, *26*, 283−291.
(23) Wiseman, T.; Williston, S.; Brandts, J. F.; Lin, L. N. *Anal. Biochem.* **1989**, *28*, 131−137.
(24) Turnbull, W. B.; Daranas, A. H. *J. Am. Chem. Soc.* **2003**, *125*, 14859−14866.
(25) Timm, D. E.; Baker, L. J.; Mueller, H.; Zidek, L.; Novotny, M. V. *Protein Sci.* **2001**, *10*, 997−1004.

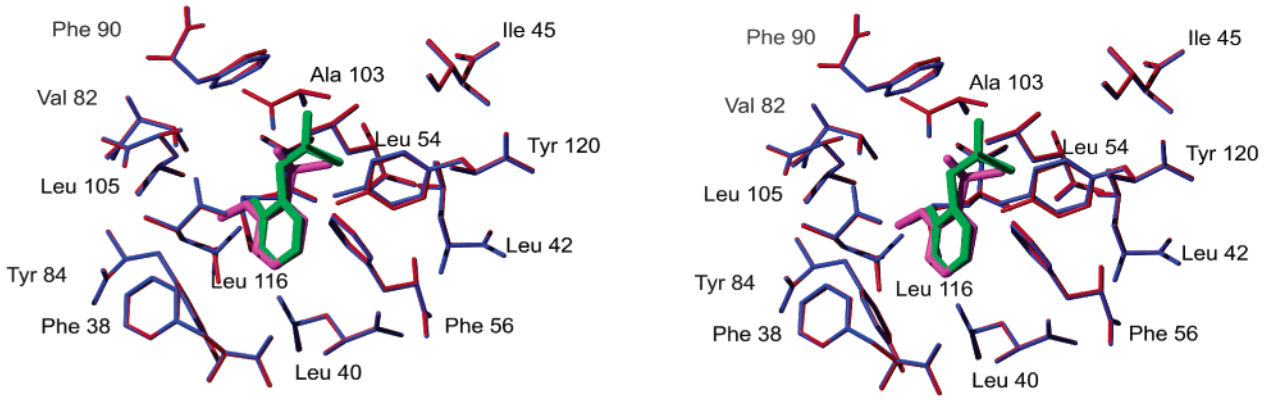

Figure 1. Stereoview of the superimposition of the ligand binding sites observed in crystal structures of complexes of MUP-I with IPMP (magenta) and IBMP (green). Binding-site residue side chains in the isopropylpyrazine complex are colored blue, and those in the isobutylpyrazine complex are colored red. Figure prepared using MOLMOL.[26]

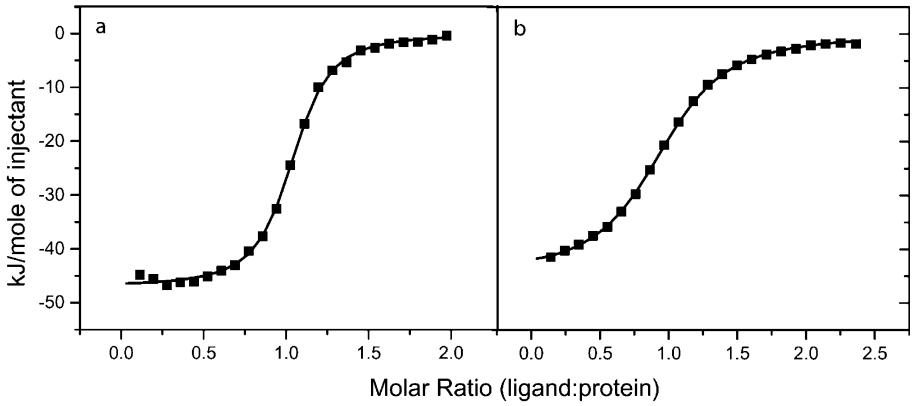

Figure 2. ITC isotherms for the binding of IBMP (left) and IPMP (right) to MUP-I.

Table 2. Thermodynamic Parameters for the Binding of IPMP and IBMP to MUP-I Derived from ITC Experiments at 308 K

ligand	$\Delta H°$ kJ/mol[a]	stoichiometry	$T\Delta S°$ kJ/mol	$\Delta G°$ kJ/mol	K_d μM
IPMP	-44.54 ± 0.4[b]	0.97 ± 0.02	-10.65 ± 0.49	-33.9 ± 0.28	1.80 ± 0.2
IBMP	-47.89 ± 0.86	1.01 ± 0.02	-9.39 ± 0.87	-38.5 ± 0.11	0.30 ± 0.01

[a] Values are expressed as the mean of two measurements. [b] Errors were determined from duplicate experiments by error propagation.

side-chain methyl groups in MUP-I both for the free protein and for complexes with IPMP and IBMP.

Backbone ^{15}N longitudinal and transverse relaxation rates ($R_1 = 1/T_1$ and $R_2 = 1/T_2$, respectively) were determined for the free protein and the complex with IBMP using uniformly ^{15}N,^{13}C(>97%),^{2}H(50%)-enriched MUP-I. Since significant shift differences exist in the complex (principally for residues within the binding site), amide ^{15}N and ^{1}H^{N} resonance assignments were determined by use of conventional three-dimensional triple-resonance experiments[27,28] (Perazzolo et al., unpublished data). In total, R_1 and R_2 data were obtained for 82 amide positions, subject to the requirement for nonoverlapping resonances in both complexes and apo protein. Shown in Figure 3 is a plot of the entropic contribution to binding ($T\Delta S^{P}_{amide}$) from the backbone for the IBMP complex, from which it is apparent that $T\Delta S^{P}_{amide}$ is statistically significant only for a minority of amide positions. Both positive and negative changes in local entropy are observed, and $T\Delta S^{P}_{amide}$ summed over backbone amides is -7.4 ± 6.5 kJ/mol, i.e. overall the backbone becomes less mobile upon ligand binding, leading to an unfavorable entropic contribution to the free energy of binding. This result is in marked contrast to that reported by Stone and co-workers for the interaction between MUP-I and 2-*sec*-butyl-4,5-dihydrothiazole, where an overall increase in backbone mobility was observed.[9] Notably, changes in backbone dynamics are not restricted to residues near the binding site. However, changes distal to the binding site are generally located in loop regions, in particular surrounding a cluster of residues located in the loop centered on Asp 98.

Side-Chain Methyl ^{2}H Relaxation Measurements. Side-chain methyl ^{2}H relaxation measurements were determined in $^{13}CH_2D$ isotopomers for both the free protein and the IBMP complex. The advantages of ^{2}H as the reporter nucleus have been discussed at length by Muhandiram et al.[8] It should be noted that resonance overlap in the methyl region of the spectrum of apo-MUP-I and its complexes is severe, and the ^{2}H relaxation properties of only a limited number of side-chain methyl groups could be obtained with accuracy (22 methyl-containing residues represented from a total of 53). However, this included all methyl-containing residues adjacent to the ligands within the binding pocket. Shown in Figure 4 are plots of $T\Delta S^{P}_{methyl}$ for side-chain methyl groups in MUP-I that were simultaneously free from resonance overlap in the free protein and the IBMP complex. It is immediately apparent that methyl-containing side chains lining the binding pocket experience a decrease in mobility on ligand binding, which consequently contributes unfavorably to affinity. However, a number of other

(26) Koradi, R.; Billeter, M.; Wuthrich, K. *J. Mol. Graphics* **1996**, *14*, 51.
(27) Ikura, M.; Kay, L. E.; Bax, A. *Biochemistry* **1990**, *29*, 4659−4667.
(28) Sattler, M.; Schleucher, J.; Griesinger, C. *Prog. Nucl. Magn. Reson. Spectrosc.* **1999**, *34*, 93−158.

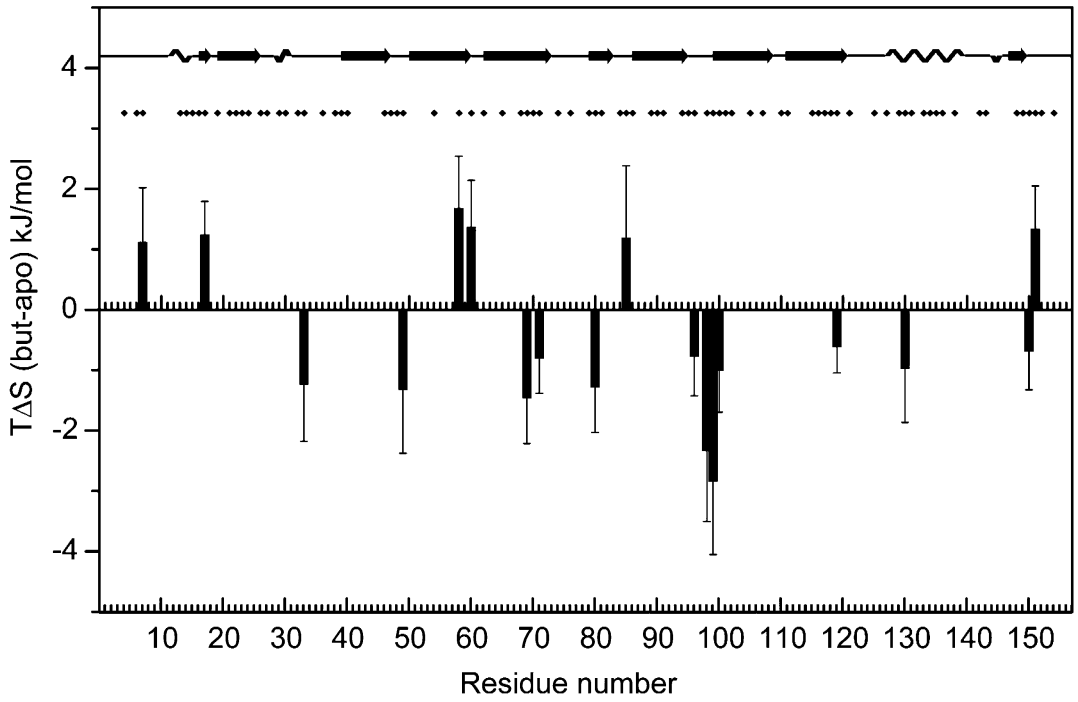

Figure 3. Plot of the entropic contribution to binding ($T\Delta S_{amide}$) of IBMP to MUP-I derived from backbone ^{15}N relaxation measurements. Error bars correspond to the propagated standard error, and data are plotted only for those residues where the absolute value of $T\Delta S_{amide}$ is greater than the standard error. Diamonds represent residues for which ^{15}N relaxation data were measured, and the secondary structure of the protein (derived from PROCHECK[22]) is also shown.

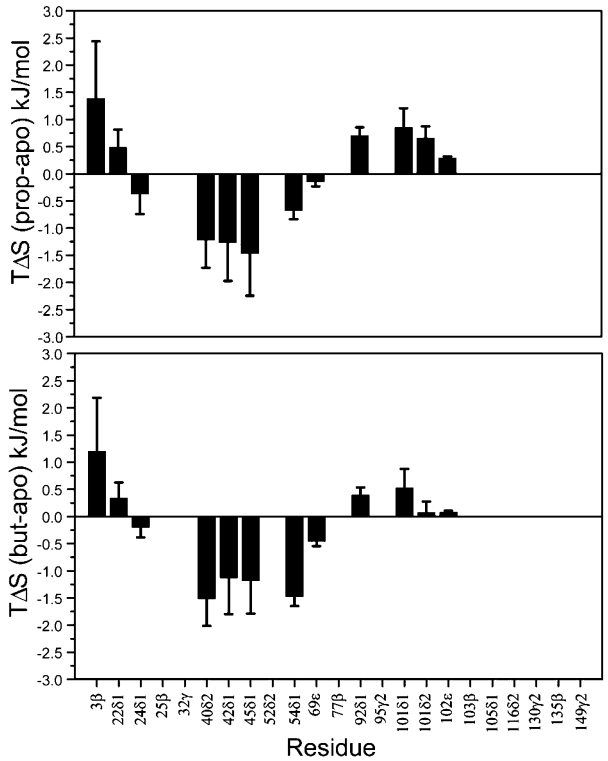

Figure 4. Plots of the entropic contribution to binding ($T\Delta S_{methyl}$) of IPMP (above) and IBMP (below) to MUP-I derived from side-chain methyl ^2H relaxation measurements. Error bars correspond to the propagated standard error, and data are plotted only for those residues where the absolute value of $T\Delta S_{methyl}$ is greater than the standard error in either complex.

residues that are distal to the binding site become more mobile on ligand binding, thus partially offsetting this unfavorable contribution. Overall, $T\Delta S^{P}_{methyl}$ for IBMP summed over all observable methyl side-chain positions is small and negative (-3.35 ± 2.77 kJ/mol).

To gain some insight into the thermodynamic basis of the specificity of MUP-I for IBMP and IPMP, side-chain methyl ^2H relaxation data were also acquired for the complex of IPMP with MUP-I. The resulting $T\Delta S^{P}_{methyl}$ values are also shown in Figure 4. The overall $T\Delta S^{P}_{methyl}$ for binding of IPMP summed over observable methyl side-chain positions is zero within experimental error (-0.77 ± 3.8 kJ/mol). The difference between this value and that for the IBMP−MUP-I complex derives principally from side chains that are proximal to the isobutyl side chain, namely Leu 54, Ile 92, and Leu 101, all of which experience decreased mobility as a consequence of the bulkiness of the isobutyl side chain of IBMP in comparison with IPMP.

Discussion

For the purposes of this discussion, the thermodynamics of the interaction between the pyrazine ligands under study and their interaction with MUP-I can be decomposed into three terms: (i) contributions arising from changes in structural and dynamic properties of the protein and ligand, including loss of translational and rotational entropy of the ligand (due to the logarithmic relationship between translational and rotational entropy and particle mass, ligand binding involves a loss of such entropy equivalent to that of the smaller particle), (ii) the free energy contribution arising from new ligand−protein interactions, and (iii) desolvation of the ligand and binding pocket on formation of the complex. The above NMR relaxation data offer insight into the contribution from the protein in (i). Figure 5 summarizes the effects on backbone and side-chain dynamics induced by binding of IBMP.

It is clear that in general there is no correlation between backbone and side-chain dynamics, as observed in a previous

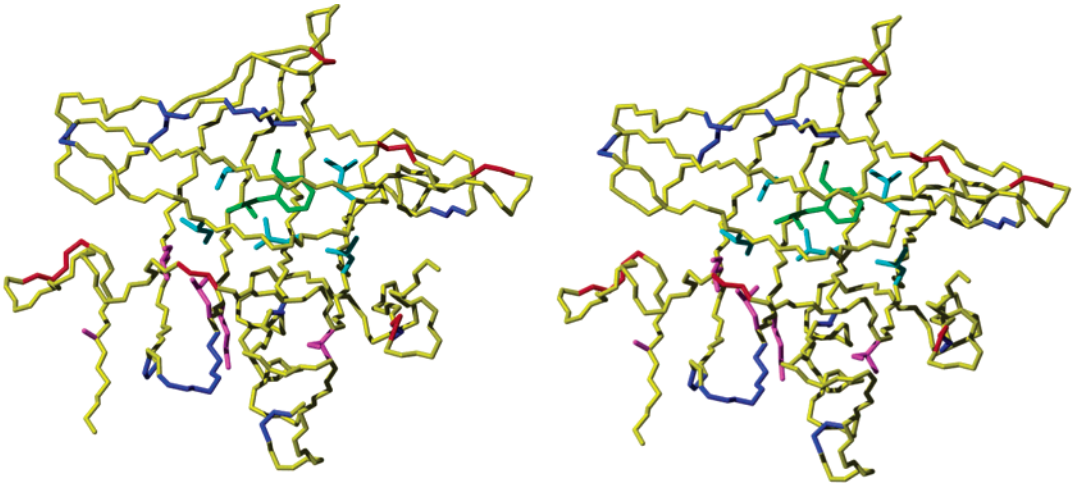

Figure 5. Structural details of residues that contribute to the entropy of binding of IBMP to MUP-I. Backbone residues that exhibit an unfavorable entropic contribution to binding are colored blue, while those that exhibit a favorable contribution are colored red. Similarly, residues whose methyl-containing side chains exhibit an unfavorable contribution are colored light blue, whereas those that exhibit a favorable contribution are colored magenta.

study on a calmodulin−peptide complex.[5] While the decreased mobility of side-chain residues within the binding pocket on binding IPMP and IBMP is hardly surprising, the concomitant increase in dynamics of side chains more distal to the binding pocket is unexpected. The dynamic changes observed in the backbone are in general located in, or adjacent to, loop regions in the protein. In particular, residues 96−100 appear to "stiffen" and hence collectively contribute a significant unfavorable entropic contribution to binding, which is partially offset by favorable entropic contributions from the adjacent side chains of Ala 3, Ile 92, and Leu 101. Taken together, these data suggest a "conformational relay" mechanism whereby increased rigidity of some residues on ligand binding gives rise to increased conformational freedom of side chains in adjacent positions, thereby overcoming in part the unfavorable entropic contribution. The overall entropy of binding, summed over backbone and side-chain positions for which data were obtainable in this study ($T\Delta S^{P}_{amide} + T\Delta S^{P}_{methyl}$), is -10.75 ± 7.1 kJ/mol for the IBMP complex. Since data available for side-chain positions is limited, this value may not represent the total contribution to $T\Delta S$ for binding from all protein degrees of freedom. Furthermore, the data only represent entropic contributions from motions on limited time scales. However, since the principal contribution to binding derives from binding-site residues, which are accessible in this study, it is reasonable to conclude that the overall internal entropic contribution to binding from internal protein degrees of freedom is unfavorable in both complexes. Similarly, it is anticipated that the contribution to the entropy of binding from the ligand will also be negative, since the internal degrees of freedom of the alkyl side chains will be restricted on binding, and the restriction in rotational and translational entropy ($T\Delta S^{L}_{T+R}$) must be overcome. Although no quantitative measurement of ligand thermodynamics was obtained in the present study, a number of previous studies have suggested bounds for these parameters, as reviewed recently by Lundquist and Toone.[29] The contribution of $T\Delta S^{L}_{T+R}$ to the free energy of binding has been estimated between −9 and −60 kJ/mol, and the rotational entropy of a completely unrestrained rotor ($T\Delta S^{L}_{rot}$) is ∼6 kJ/mol. Thus, the overall unfavorable entropic contribution to binding of IBMP summed over ligand degrees of freedom can be estimated as $T\Delta S^{L}_{T+R} + T\Delta S^{L}_{rot} = -27$ to -78 kJ/mol, assuming that methyl rotors are completely unrestrained on binding and all other rotors are completely restrained on binding in IBMP.

With regard to solvation effects (iii, above) since both IPMP and IBMP are predominantly hydrophobic, as is the binding pocket of MUP, intuitively one would anticipate that binding would be dominated by the classical hydrophobic effect. This is characterized by a positive $T\Delta S$ due to release of ordered water molecules from the protein and ligand into bulk solvent and a large negative change in heat capacity.[30−32] However, the above ITC data clearly show negative $T\Delta S$ values, and $\Delta H°$ values that are essentially independent of temperature over the range 300−308 K (data not shown). In a recent study, Stone and co-workers determined the global thermodynamics of binding of the pheromone derivatives isobutyl-4,5-dihydrothiazole (IBT) and isopropyl-4,5-dihydrothiazole (IPT) to MUP-I[33] and obtained $\Delta H° \approx -52$ kJ/mol, $T\Delta S° \approx -14.8$ kJ/mol for IBT and $\Delta H° \approx -50$ kJ/mol, $T\Delta S° \approx -19.3$ kJ/mol for IPT, at 308 K. In this same study, the thermodynamics of desolvation of the MUP-I ligand 2-*sec*-butyl-4,5-dihydrothiazole (SBT) was determined using classical solvent-partitioning experiments, giving rise to an unfavorable enthalpic contribution ΔH^{L}_{solv} of ∼4 kJ/mol, and a favorable entropic contribution $T\Delta S^{L}_{solv}$ of 7.5 kJ/mol. Given the similarity between SBT, IPMP, and IPMP it is reasonable to assume that solvation thermodynamics of IPMP and IBMP are of similar magnitude. With regard to protein solvation, the complex studied by Stone and co-workers[25] contains two bound water molecules in the binding site (Figure 6). In contrast, the IBMP−MUP-I and IPMP−MUP-I complexes examined in the present study do not contain any bound water molecules (Figure 6)—the presence of the methoxy group and the more bulky pyrazine scaffold results in a displacement of the ligand toward the position occupied by the bound waters, and Tyr 120 hydrogen bonds directly to IBMP, rather than via the bound waters as in the IBT complex. Thus, assuming similar thermodynamics for the thiazole and

(29) Lundquist, J. J.; Toone, E. J. *Chem. Rev.* **2002**, *102*, 555−578.

(30) Blokzijl, W.; Engberts, J. *Angew. Chem., Int. Ed. Engl.* **1993**, *32*, 1545−1579.
(31) Muller, N. *Acc. Chem. Res.* **1990**, *23*, 23−28.
(32) Privalov, P. L.; Gill, S. J. *Adv. Protein Chem.* **1988**, *39*, 191−234.
(33) Sharrow, S. D.; Novotny, M. V.; Stone, M. J. *Biochemistry* **2003**, *42*, 6302−6309.

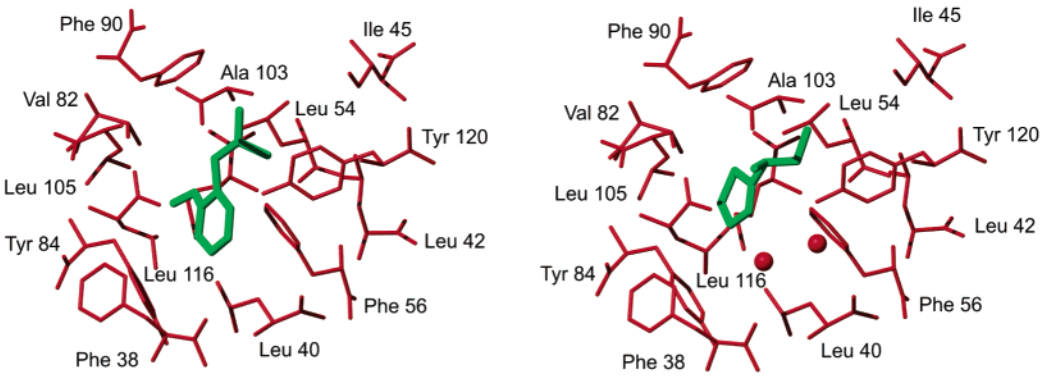

Figure 6. Details of the binding site from the crystal structure of (left) IBMP−MUP-I complex described in the present study and (right) isobutyl-4,5-dihydrothiazole (IBT)−MUP-I complex described by Timm et al.[25] Bound water molecules are illustrated as spheres.

Table 3. Contributions to the Entropy of Binding of IBMP to MUP

entropic contribution	value (kJ/mol)	value (kJ/mol) ITC
protein degrees of freedom $T\Delta S^{P}_{amide} + T\Delta S^{P}_{methyl}$	-10.75 ± 7.1	−
ligand degrees of freedom $T\Delta S^{L}_{T+R} + T\Delta S^{L}_{conf}$	−27 to −78	−
ligand solvation $T\Delta S^{L}_{solv}$	+7.5	−
protein solvation $T\Delta S^{P}_{solv}$	+24	−
entropy of binding $T\Delta S_b$	−64 to +1	-9.39 ± 0.87

pyrazine ligands in free solution, a comparison of the thermodynamic data for the thiazole and pyrazine complexes suggests that the entropic contribution from the release of a bound water molecule $T\Delta S^{P}_{solv}$ is +3−4 kJ/mol, which is within the bounds of at most ca. 8 kJ/mol per water molecule proposed by Dunitz.[34] To date, all reported crystal structures of MUP-I contain an endogenous ligand (including the structure reported in the present study), and hence, an experimental measure of the number of water molecules in the binding pocket is not available. However, by use of the program PRO_ACT [35] with a probe radius of 0.14 nm, together with the crystal structure of the IBMP complex reported here, we estimate that a maximum of six water molecules are displaced on ligand binding, giving rise to a total $T\Delta S^{P}_{solv}$ of $<+24$ kJ/mol.

While the above analysis is clearly only semiquantitative in view of the numbers of inherent approximations, these data, which are gathered in Table 3, clearly suggest that ligand binding to MUP-I is not driven by the classical hydrophobic effect. Gratifyingly, the global value of $T\Delta S_b$ derived from ITC measurements is within the bounds suggested by the above analysis and suggests that the entropic contribution from ligand degrees of freedom ($T\Delta S^{L}_{T+R} + T\Delta S^{L}_{conf}$) is at the lower end of the range (ca. −30 kJ/mol) reported in the literature (reviewed by Lundquist and Toone[29]). This corresponds with $T\Delta S^{L}_{T+R} =$ 12 kJ/mol for IBMP (using the same assumptions regarding the mobility of ligand rotors described above) which is in reasonable agreement with the value of 25.8 kJ/mol determined experimentally for the binding of oligosaccharide fragments binding to cholera toxin,[36] given the logarithmic dependence of this parameter with molecular mass.

Finally, we refer to the observed selectivity of MUP-I, i.e. its preference for IBMP versus IPMP. The entropic contribution to binding of IPMP from internal protein degrees of freedom ($T\Delta S^{P}_{amide} + T\Delta S^{P}_{methyl}$) is more favorable than for IBMP (see above). Similarly, the entropic contribution to binding of IPMP from ligand degrees of freedom ($T\Delta S^{L}_{T+R} + T\Delta S^{L}_{conf}$) would be expected to be more favorable by ∼6 kJ/mol due to the reduction in the number of degrees of freedom in IPMP in comparison with those in IBMP (the contribution from $T\Delta S^{L}_{T+R}$ remaining essentially constant in both cases). Moreover, since the crystal data obtained in the present study show no evidence for bound water molecules in either the IPMP−MUP-I or IBMP−MUP-I complexes, then clearly the greater affinity of IBMP for MUP-I in comparison with IPMP cannot be explained by a difference in solvation of the binding site in the complex. The slightly more favorable $T\Delta S_b$ observed for IBMP in comparison with IPMP from ITC studies (Table 2), therefore, is likely to derive from a favorable entropic contribution from ligand solvation ($T\Delta S^{L}_{solv}$) that more than compensates the unfavorable terms just described.

In both complexes under study, binding is enthalpy driven and hence is not driven by the classical solvent-driven hydrophobic effect. Since only one ligand−protein hydrogen bond is observed in either complex, the principal driving force for binding can be attributed to solvent-driven enthalpic effects,[37] as has been reported for the related lipocalin porcine odorant binding protein.[38] By use of solvent isotope effect measurements, Chervenak and Toone concluded that 25−100% of the net measured enthalpy of binding in biomolecular complexes is accounted for by solvent reorganization.[39] The results obtained here are compatible with this conclusion. However, the unfavorable enthalpic contribution to ligand desolvation ΔH^{L}_{solv} of ∼4 kJ/mol measured by Stone and co-workers for IPT[33] suggests that the dominant contribution to the enthalpy of binding is driven by water molecules released from the protein binding pocket. These thermodynamic effects should be detectable in solvent isotopic substitution experiments which are in progress.

Acknowledgment. This work was supported by BBSRC, Grants 24/B12992 and 24/B19388 to S.W.H. and 24/SB11269 to S.E.V.P., by The Wellcome Trust grant number 062164, and by the Fonds National de la Recherche Scientifique et l'Innovation of Switzerland to G.B.

JA038461I

(34) Dunitz, J. *Science* **1994**, *264*, 670.
(35) Williams, M. A.; Goodfellow, J. M.; Thornton, J. M. *Protein Sci.* **1994**, *3*, 1224−1235.
(36) Turnbull, W. B.; Homans, S. W. *J. Am. Chem. Soc.* In press.
(37) Lemieux, R. U. *Acc. Chem. Res.* **1996**, *29*, 373−380.
(38) Burova, T.; Choiset, Y.; Jankowski, C. K.; Haertle, T. *Biochemistry* **1999**, *38*, 15043−15051.
(39) Chervenak, M. C.; Toone, E. J. *J. Am. Chem. Soc.* **1994**, *116*, 10533−10539.